

J.-Ch. ROBINET and G. CASALIS  
*ONERA-CERT*  
*2, avenue Edouard Belin, B.P. 4025*  
*31055 TOULOUSE Cedex 4, FRANCE*

**Simulated Reprint from**

**Journal of AIAA**

Volume 37, Number 4, Pages 453–459

*A publication of the*  
American Institute of Aeronautics and Astronautics, Inc.  
1801 Alexander Bell Drive, Suite 500  
Reston, VA 22091

# SHOCK OSCILLATIONS IN DIFFUSER MODELLED BY A SELECTIVE NOISE AMPLIFICATION

J.-Ch. ROBINET\* and G. CASALIS†

ONERA-CERT

2, avenue Edouard Belin, B.P. 4025  
31055 TOULOUSE Cedex 4, FRANCE

It has been observed that shock waves in supersonic flow oscillate under certain conditions. These oscillations usually have negative effects especially for flow past transonic airfoils and in supersonic diffusers. It is therefore of practical importance to understand the origin and the consequences of these oscillations. The purpose of this paper is to model and to predict some physical characteristics of self-sustained shock oscillations in transonic diffuser flows. This paper gives first the results of a quasi-one-dimensional stability analysis. The mean flow is calculated with a code solving the averaged Navier-Stokes equations. The present stability approach is however limited to the core region where the viscous effects can be neglected. In order to validate the present approach, the results are compared with Sajben's experimental data and those numerically obtained by Hsieh. As demonstrated below, the main characteristics of the oscillation are clearly obtained: for example the shock motion spectra is correctly reproduced by the present stability approach.

## Nomenclature

### Latin Alphabet

$k$	wave number
$R_p$	exit pressure to total inlet pressure ratio
$l$	diffuser length (from throat to exit)
$h$	throat height
$U, u$	streamwise velocity component
$V, v$	transverse velocity component
$T$	temperature
$a$	sound velocity
$t$	time
$X$	amplitude of shock motion

### Greek Alphabet

$\omega/2\pi$	frequency
$\rho$	density

### Subscripts

$(\cdot)_o$	upstream value
$(\cdot)_1$	downstream value
$(\cdot)_f$	fluctuation value
$(\cdot)_c$	shock value
$(\cdot)_e$	exit value

### Superscripts

$(\bar{\cdot})$	mean value
$(\cdot)$	Amplitude function for the perturbation

## Introduction

Under certain conditions, the shock wave in supersonic flows may exhibit oscillations. This occurs for example with transonic airfoils and in supersonic diffusers. Different approaches have been used in order to quantify these oscillations and to understand their physical origin. Many experiments have been carried out by Sajben<sup>1</sup> *et al.* in the beginning of 80's whereas some numerical simulations have been tried by Liou, Coakley<sup>2</sup> and Hsieh.<sup>3</sup> A new approach is proposed in this paper which is more theoretical than the two others and which can provide thereby a new insight in this difficult problem. It is more or less admitted that the geometry of the diffuser, the shock intensity, the separation bubble of the boundary layer just downstream the shock and the subsonic core region play an important role in these oscillations. But neither the experiment nor the numerical simulations can explain: "who does what, how and why".

\*PhD Student, Department Modelling Aerodynamics and Energetics, Transition and instability Group.

†Research Scientist, Department Modelling Aerodynamics and Energetics, Transition and instability Group.

Presented as Paper 98-3419 at the AIAA 34th Joint Propulsion Conference, Cleveland, OH, Jul. 13-15, 1998; received Nov. Date, Years; revision received Month. Date, Years; accepted for publication Month Date, year. Copyright ©1998 by the American Institute of Aeronautics and Astronautics, Inc. All rights reserved.

The objective is to prove by simple models that the frequency of the self-sustained oscillations at least can be predicted by a small perturbation technique based on inviscid perturbations superimposed to a viscous mean flow.

This first part describes the published results: the experimental and the numerical ones. In the second part, the theoretical aspects of a quasi-one-dimensional stability analysis are described. This approach consists in studying these oscillations using a simple linear stability analysis. This analysis is restricted to the core region where the viscous effects are negligible and, in accordance with experimental results, the mean flow is assumed to be nearly one-dimensional in this region. However, the mean flow is calculated using the code FLU3M developed at ONERA in order to obtain accurate values for the mean flow. The one-dimensional stability results are then presented in comparison with Sajben's experiments and with Hsieh numerical simulations. The results are finally compared both to experimental results and to the results provided by the previous simplified stability approach.

## 1 Background of the Present Study

### Diffuser Geometry

The major experimental contribution on self-sustained shock oscillations has been brought by the Mc Donnell Douglas team headed by M. Sajben.<sup>4,1,5</sup> One of the diffusers used in the experiment is asymmetric with a flat bottom wall and a converging-diverging channel with a maximum  $9^\circ$  divergence angle. This diffuser is equipped with many suction slots, so that the flow can be considered two-dimensional, at least in the middle section between the two lateral walls of the channel. Figure 1 gives a sketch of the experimental set-up.

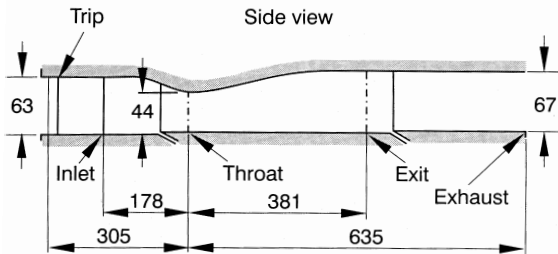


Fig. 1 Sajben *et al.* diffuser model.

The relative diffuser length is  $l/h$  where  $h$  is the height at the throat, the length origin is chosen at the throat. In this paper, only the

diffuser lengths such as  $l/h \geq 10$  are studied with the proposed approaches.

### General Descriptions

In this nozzle, the fluid accelerates from subsonic to supersonic speed through a sonic throat, and is abruptly decelerated by a shock-wave located downstream of the throat. The flow in this diffuser is exhausted directly to the ambient air so that the boundary conditions at the exit cross section are closely characterised by a spatially and temporally constant static pressure. The flow conditions are then mainly characterised by the ratio of the static pressure at the exit section to the total pressure at the inlet:  $R_p = p_e/p_t$ . This ratio determines, among other properties, the shock strength and the Mach number  $M_0$  ahead of the shock. The flow patterns obtained with this diffuser depend on the Mach number. In Sajben's experiment, shock-induced separation occurs for Mach numbers  $M_0$  greater than 1.3 and, in this case spontaneous self oscillations have been observed. These oscillations consist of a shock oscillating motion together with the occurrence of fluctuations downstream of the shock. In all cases, no oscillation has been observed in the supersonic zone. The following results are limited to one value of  $R_p$ :  $R_p = 0.72$  ( $M_0 = 1.34$ ).

### Experimental and Numerical Results

Among the Sajben's experimental results, the shock motion power spectrum is of particular interest. This spectrum<sup>4</sup> is represented in figure 2.

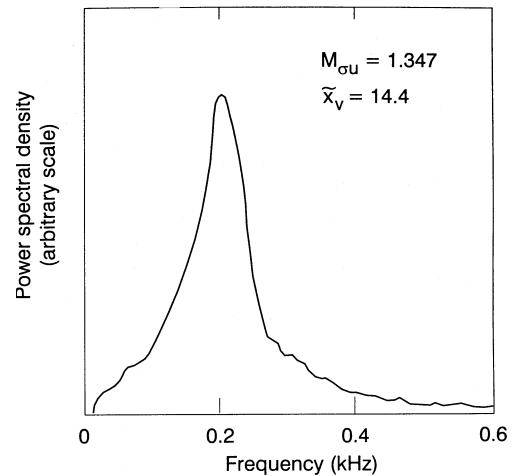


Fig. 2 Shock motion power spectrum, experiment.

It shows that the most sensitive frequencies, for a diffuser length  $l/h = 14.4$ , are close to

200 Hz. Different lengths ( $12 \leq l/h \leq 30.5$ ) have been studied by Sajben *et al.*<sup>1</sup> Computations have been performed by Coakley, Liou and Hsieh,<sup>3,6</sup> for the same diffuser configuration. These simulations consisted in solving the unsteady averaged Navier-Stokes equations with a classical turbulence model. They were achieved in two steps: steady computations provided the mean flow and then the unsteady computations determined the fluctuating quantities. These unsteady computations have been realised by imposing a fluctuating pressure at exit section. Hsieh and Coakley<sup>3</sup> used different diffuser lengths (see Table 1).

Frequency (Hz)	$l/h$ (case)
300	8.66 (A)
250	10.06 (B)
210	12.08 (C) height310
14.7 (D)	

**Table 1 Oscillation frequency for different diffuser lengths (numerical results).**

Figure 3 shows the computed shock motion power spectrum corresponding to these cases. It can be observed that when the diffuser length  $l/h$  is less than 12 the frequency of oscillation reduces from 300 to 210 Hz as the downstream boundary location varies from  $l/h = 8.6$  to 12.08, whereas the frequency increases to 310 Hz for the greatest length ( $l/h = 14.7$ ). The latter does not agree with the experimental result (198 Hz) published by Sajben<sup>1</sup> and given in figure 2.

Taking into account all these published re-

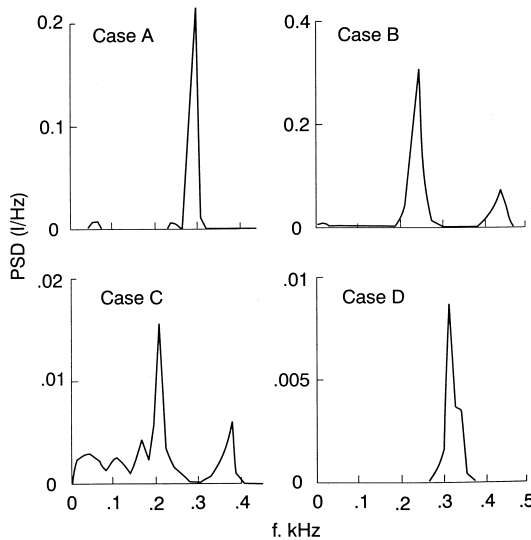


**Fig. 3 Shock motion power spectrum, Computation**

sults (experiment and numerical simulations),

the present analysis is devoted to a simpler and more analytical approach.

Let us summarize, the different diffuser lengths used in the Sajben's experiment, in Hsieh's calculation and in our present approach:

- Sajben's experiment:  $12 \leq l/h \leq 30.5$
- Hsieh's simulation:  $8.6 \leq l/h \leq 14.7$
- present approach:  $8.6 \leq l/h \leq 13$

The upper limit of  $l/h$  used in our approach ( $l/h \leq 13$ ) comes from the available mean flow computation performed in ONERA.<sup>7</sup>

## 2 Mean and Fluctuating Flows

The purpose of this section is to describe the main assumptions employed in the proposed small perturbation technique. The classical coordinate system  $(x, y)$  is used, where  $x$  is the streamwise coordinate and  $y$  is perpendicular to it.

### Small Perturbation Technique

Two present approaches are based on the standard small perturbation technique. The instantaneous flow is written as the superposition of a basic flow and of a small fluctuation. All physical quantities  $q$  (velocity, pressure, ...) are thus decomposed into a mean value and a fluctuating one :

$$q = \bar{q} + q_f. \quad (1)$$

The physical quantities related to the mean flow are overlined; for example,  $\bar{U}$  is the mean streamwise velocity component.

### Mean Flow Calculation

The mean flow comes from a computation. The code **FLU3M**<sup>8</sup> developed at **ONERA** solves the average Navier-Stokes equations, a Jones-Launders  $k-\varepsilon$  model has been used. This computation is similar in principle to the first step of the numerical simulation done by Liou *et al.*<sup>6</sup> This model allows a good representation of the shock-boundary layer interaction.<sup>9</sup> Before describing the formalism of the proposed model, we must first check that the computed mean flow is in agreement with Sajben's experimental results.

The two different grids has been used for the computation of the mean flow. The first one

consists in a (136x99) grid with a fine distribution of points only near the upper and lower walls in order to have enough points in the boundary layers. In the  $x$  direction, the mesh is strengthened around the expected shock wave location. The second computational grid (136x111 points) is refined in the  $y$ -direction in the central zone of the diffuser in order to compute the evolution in the  $y$ -direction of mean flow more accurately. Figures 5 and 6 show the experimental and

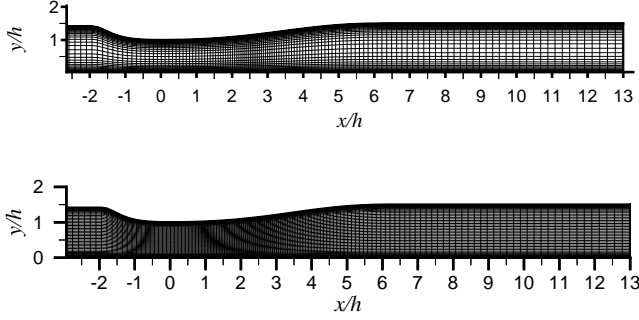


**Fig. 4 The two different grids**

numerical results respectively for the iso- $\bar{U}$  contours. From these results, it can be concluded that both computed mean flows are in good agreement with the experimental data. However, a detailed study shows that small differences still exist just downstream of the shock and between the  $y$ -derivative of the different mean flow quantities.

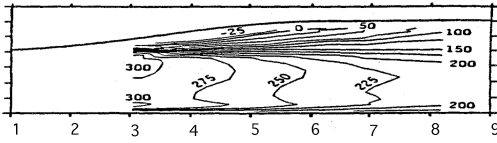


**Fig. 5  $\bar{U}$  contours (m/s), experiment**

An instructive behaviour is provided by the evolution of the longitudinal mean velocity in the  $x$  direction (and in the middle of the core flow), see figure 7. It can be observed that instead of a continuous decrease up to exit section, the mean flow increases just downstream of the shock before to decreasing. This expansion effect results from the large separation bubble in the upper boundary layer. The boundary layers separation generates a local acceleration. This characteristic is present only in the middle of the diffuser which is not obtained by solving the steady invicid equations. The experimental checking of this assumption, could not be made because of a lack of experimental data in this configuration (in the core

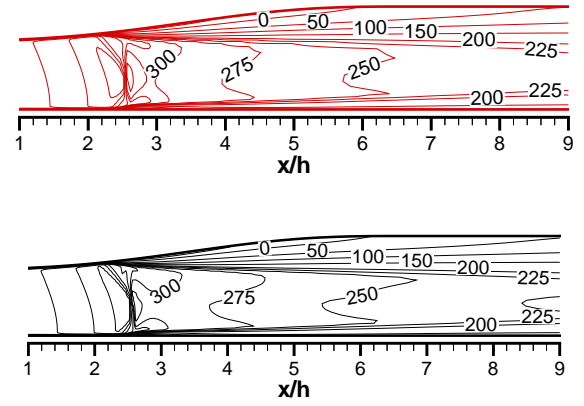


**Fig. 6  $\bar{U}$  contours (m/s), computation. Top : (136x99) points, bottom : (136x111) points**

of the diffuser, for  $R_p = 0.72$ ). This local acceleration may be however the origin of the shock oscillation. For many years, it is well known that the shock is unstable in a converging nozzle (i.e. when the flow accelerates).<sup>10</sup> It must

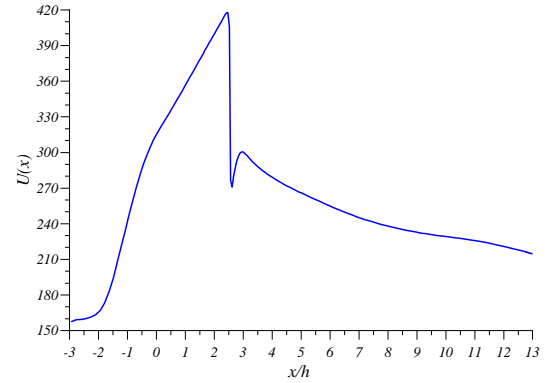


**Fig. 7 Mean flow evolution, core flow.**

be pointed out that subsequently the proposed approaches will take into account the separated region, but only through the mean flow values. So in these approaches, the boundary layer and its separated region are considered as steady.

### Basic Equations for the Small Perturbation Technique

The equations for the instantaneous flow are the Euler equations, the energy equation written for the total enthalpy and the equation of perfect gas. The proposed approaches are thus limited to the core region where the viscous effects can be neglected.

- Equation of continuity:

$$\frac{\partial \rho}{\partial t} + \frac{\partial(\rho U)}{\partial x} + \frac{\partial(\rho V)}{\partial y} = 0, \quad (2)$$

- $x$ -momentum equation :

$$\rho \frac{\partial V}{\partial t} + \rho U \frac{\partial V}{\partial x} + \rho V \frac{\partial V}{\partial y} + \frac{\partial P}{\partial x} = 0, \quad (3)$$

- $y$ -momentum equation :

$$\rho \frac{\partial V}{\partial t} + \rho U \frac{\partial V}{\partial x} + \rho V \frac{\partial V}{\partial y} + \frac{\partial P}{\partial y} = 0, \quad (4)$$

- Enthalpy equation :

$$\rho \frac{\partial h_i}{\partial t} + \rho U \frac{\partial h_i}{\partial x} + \rho V \frac{\partial h_i}{\partial y} = \frac{\partial P}{\partial t}, \quad (5)$$

- Total enthalpy definition :

$$h_i = C_p T + \frac{U^2 + V^2}{2}, \quad (6)$$

- Equation of state :

$$P = r \rho T, \quad (7)$$

where  $r$  and  $C_p$  are respectively the perfect gas constant ( $r = 287 \text{ m}^2 \text{ s}^{-2} \text{ K}^{-1}$ ) and specific heat coefficient ( $C_p = 1007 \text{ m}^2 \text{ s}^{-2} \text{ K}^{-1}$ ).

The instantaneous flow also depends on of the Rankine-Hugoniot relations written at the instantaneous location of the shock :

$$\rho_1 (V_{n1} - W_c) = \rho_0 (V_{n0} - W_c), \quad (8)$$

$$P_1 + \rho_1 (V_{n1} - W_c)^2 = P_0 + \rho_0 (V_{n0} - W_c)^2, \quad (9)$$

$$V_{\tau 1} = V_{\tau 0}, \quad (10)$$

$$C_p T_1 + \frac{1}{2} (V_{n1} - W_c)^2 = C_p T_0 + \frac{1}{2} (V_{n0} - W_c)^2, \quad (11)$$

where  $V_n$  is the velocity component normal to the shock,  $V_\tau$  is the tangential component and  $W_c$  is the velocity of the shock front.

### 3 Stability Analysis

The decomposition (1) is first introduced into equations (2) to (7). The mean flow, which satisfies the Navier-Stokes equations, is assumed to be a solution of the inviscid equations in this region. The resulting equations are further simplified by considering that the perturbation is small, so that the nonlinear fluctuating terms can be neglected.

Finally, equations (2) to (7) are transformed into a linear system, the coefficients of which are functions of the mean flow.

**Perturbation Form**  
According to the experimental and numerical results, the mean flow in the core region is assumed to be weakly dependent on  $y$ , so that any mean quantity verifies the relation :

$$\partial \bar{q} / \partial y \ll \partial \bar{q} / \partial x, \quad \forall x, \forall y. \quad (12)$$

With this assumption, a perturbation can be sought with a uniform exponential dependence with respect to  $y$ . Thus any fluctuating quantity is written as :

$$q_f(x, y, t) = \Re [\tilde{q}(x) \cdot e^{\omega_i t} \cdot e^{i(ky - \omega_r t)}], \quad (13)$$

where  $\tilde{q}$  is a complex function,  $k$  is a real wave number and  $\omega_i$  is a temporal amplification rate, whereas the real part  $\omega_r$  of  $\omega$  characterises the frequency of the perturbation.  $\Re(z)$  is the real part of  $z$ . The linear stability of the flow depends on the sign of  $\omega_i$ : for  $\omega_i < 0$  the mean flow is linearly stable, whereas for  $\omega_i > 0$  the mean flow is unstable. The  $y$ -dependence is justified by the fact that the mean flow is not exactly one-dimensional. There is a transverse velocity  $\tilde{V}$  such as  $\max(\tilde{U}/\tilde{V}) \simeq 5.10^{-2}$ . In order to be coherent with symetries of the problem the perturbation must be two-dimensional ( $k \neq 0$ ).

#### Stability Equations and Boundary Conditions

With the perturbation (13), the linearized Euler equations become an ordinary fourth-order differential system :

$$\mathbf{C} \frac{d\mathbf{Z}}{dx} = \mathbf{B}\mathbf{Z}, \quad (14)$$

where  $\mathbf{Z}(x)$  is the amplitude function vector of the perturbation. Its components are  $\tilde{T}, \tilde{\rho}, \tilde{u}, \tilde{v}$ , which denote respectively the fluctuating temperature, the density and the longitudinal and transverse velocities components.  $\mathbf{C}$  and  $\mathbf{B}$  are two  $(4, 4)$  complex matrices which are functions of the mean flow and of the coefficients  $\omega$  and  $k$ .<sup>11</sup>

In all the tested experimental configurations, no fluctuation has been observed in the supersonic zone flow. For this reason, the first boundary condition is chosen as :

$$\mathbf{Z}(0) = 0, \quad (15)$$

This means that there is no fluctuation at the throat. In exit section, the fluctuations do not necessarily vanish. It is only imposed that the perturbations are bounded at the exit section:

$$\|\mathbf{Z}(l/h)\| \ll \infty. \quad (16)$$

The differential system (14)-(16) has  $\mathbf{Z} \equiv 0$  as natural and trivial solution. Moreover it is the only one unless the problem becomes singular. In fact, the determinant of the matrix  $C$  is always invertible except at the position defined by  $\bar{M} = 1$ . The problem is thus regular from throat to shock. Then, according to the boundary condition (15),  $\mathbf{Z} \equiv 0$  is the only solution of the problem upstream of the shock: in the whole supersonic zone there is no fluctuation. However, if the system of equations (14) is singular at the mean shock position, another solution (i.e. not trivial) may exist. To find this solution, a special procedure needs to be used at the shock position. This procedure is obtained with the shock relations (8) to (11).

### Linearised Shock Relations

According to the small perturbation technique (1) and expression (13), the perturbed position of the shock is written as :

$$x = \bar{x}_c + \Re [X e^{i(ky - \omega t)}]. \quad (17)$$

In (17),  $\bar{x}_c$  represents the mean shock position ( $\bar{x}_c/h \simeq 2.6$ ) and  $X$  the amplitude of the shock displacement which is assumed to be a small quantity. The Rankine-Hugoniot equations (8) to (11) are then linearized by performing a first order Taylor expansion with respect to  $X$ . The quantities downstream of the shock are denoted by subscript 1 and those upstream of the shock by subscript 0. In fact, all quantities  $q$  ( $q_1$  or  $q_0$ ) are the sum of the mean and of the fluctuating values evaluated just downstream for ( $q_1$ ) or upstream for ( $q_0$ ) of the perturbed position of the shock:

$$q(x, y, t) = \bar{q}(\bar{x}_c + XE) + q_f(\bar{x}_c + XE),$$

where  $E = e^{i(ky - \omega t)}$ .

After expansion,  $q_1$  is written as :

$$q_1(x, y, t) = \bar{q}_1(\bar{x}_c) + \frac{\partial \bar{q}_1}{\partial x}(\bar{x}_c)XE + \tilde{q}_1(\bar{x}_c)E.$$

As there is no fluctuation upstream of the shock,  $q_0$  is simply given by:

$$q_0(x, y, t) = \bar{q}_0(\bar{x}_c) + \frac{\partial \bar{q}_0}{\partial x}(\bar{x}_c)XE.$$

It can be noted that in the previous expression the derivative of  $\bar{q}_0$  with respect to  $x$  corresponds to the left derivative (in  $x_0^-$ ); the same

is true for the  $x$  derivative of  $\bar{q}_1$  and the right derivative (in  $x_0^+$ ). After some calculation, the linearized shock relations lead to an algebraic system of equations:

$$A\mathbf{Z}(\bar{x}_c) = \xi X, \quad (18)$$

where  $\mathbf{Z}(\bar{x}_c)$  is the vector of the fluctuating amplitudes calculated at  $\bar{x}_c$ ,  $\xi$  is a complex vector and  $A$  is a fourth-order complex matrix;  $A$  and  $\xi$  are known. From another point of view, it should be noted that the behaviour of mean flow on both sides of shock (for example : the local convergent effect indicated in figure 7) occurs in the term  $\xi$  through the right and left derivatives of the mean flow. Finally, as the matrix  $A$  is invertible,<sup>11</sup> the vector  $\mathbf{Z}$  at the mean shock position is known:

$$\mathbf{Z}(\bar{x}_c) = A^{-1}X\xi. \quad (19)$$

All fluctuating quantities are thereby proportional to the shock oscillation amplitude  $X$ , which cannot be determined within the linear stability analysis.

### Summary

The stability problem has been easily solved in the supersonic zone,  $\mathbf{Z} = 0$  is the unique solution. In the subsonic zone, the system (14) with the boundary conditions (15) and (16) is an eigenvalue problem. The trivial solution  $\mathbf{Z} \equiv 0$ ,  $X = 0$  is a solution. A non-zero solution can exist only if the problem is singular, which implies a particular choice of the wave number  $k$  and of the complex circular frequency  $\omega$  of the perturbation. This choice corresponds to a dispersion relation between these numbers, which cannot be determined analytically. In the following, a numerical procedure devoted to this point is described.

### Analytical study

If the mean flow is considered as uniform i.e. independent of  $x$ , the differential system (14) becomes a linear differential system with constant coefficients. Then an analytical solution can be calculated:

$$\mathbf{Z}(x) = \sum_{j=1}^4 c_j \mathbf{Z}_j(x) \text{ with } \mathbf{Z}_j(x) = \mathbf{V}_j e^{l_j x}, \quad (20)$$

where the coefficients  $c_j$  are unknown integration constants, which will be determined by

the boundary conditions.  $v_j$  and  $\mathbf{V}_j$  are respectively the eigenvalues and eigenvectors of matrix  $\mathbf{C}^{-1}\mathbf{B}$ , see (14). The expressions of  $l_j$  and  $\mathbf{V}_j$ <sup>11</sup> are given in the appendix. Physically, the first two modes ( $j = 1, 2$ ) correspond to the acoustic modes, respectively the downstream and upstream travelling waves, and the other two modes ( $j = 3, 4$ ) correspond to the entropic and the rotational modes which are convected with the mean flow. In order to verify the condition (16), these different modes  $\mathbf{V}_i e^{l_i x}$  cannot exhibit an exponentially increasing behaviour:  $\Re(l_i) \leq 0$  where  $\Re(l_i)$  denotes the real part of  $l_i$ . It can be shown that  $\Re(l_3) \leq 0$  if  $\omega_i \geq 0$ ,  $\Re(l_2) \leq 0$  and  $\Re(l_1) \geq 0$  for all  $\omega$  and  $k$ . Nevertheless, when  $\omega_i \leq 0$ ,  $\mathbf{V}_3 e^{l_3 x}$  and  $\mathbf{V}_4 e^{l_4 x}$  are smaller than  $\mathbf{V}_2 e^{l_2 x}$ , it can be then considered that the only one not acceptable mode with respect to boundary condition (16) is  $\mathbf{V}_1 e^{l_1 x}$ . The relation  $c_1 = 0$  must be imposed. This relation amounts to the assumption that there are no downstream travelling waves; this is finally in agreement with Culick and Rogers's theory.<sup>12</sup> According to the latter, the reflected downstream travelling wave amplitude is about 6 times smaller than the upstream travelling wave amplitude (in the case of the mean flow described in section (2)). The general solution is written as :

$$\mathbf{Z}(x) = c_2 \mathbf{Z}_2(x) + c_3 \mathbf{Z}_3(x) + c_4 \mathbf{Z}_4(x), \quad (21)$$

However according to figure 7, there is no evidence of the presence of any uniform zone, but, at a certain distance from the shock, it is assumed that the mean flow does not depend too much on  $x$ . In this "uniform zone", for  $x \geq x_u$  ( $x_u/h \simeq 11$ ), the solution of (14) can be written as (21). Equation (14) is then numerically integrated for each vector  $\mathbf{Z}_j$  ( $j=2,3,4$ ) by decreasing values of  $x$  from the uniform zone boundary  $x_u$  up to the mean shock position  $\bar{x}_c$ . At this position, there are two formulations of  $Z(x)$ ; the first one comes from the numerical integration and equation (21) and the second one is simply given by the boundary condition (19). These two expressions should coincide. For a given circular frequency  $\omega_r$ , the unknowns are the complex constants  $c_2, c_3, c_4$ . These six real unknowns are searched in order to verify the following relationship :

$$\mathbf{Z}(\bar{x}_c) = c_2 \mathbf{Z}_2(\bar{x}_c) + c_3 \mathbf{Z}_3(\bar{x}_c) + c_4 \mathbf{Z}_4(\bar{x}_c),$$

which provide four scalar complex relations. A non zero solution only can exist if the rank of

this system of four relations is only three. This condition is a dispersion relation: it is satisfied with a particular value of  $(k, \omega_i)$  for a given value of frequency  $\omega_r/2\pi$  of the perturbation. A trial and error method is finally used to determine the eigenvalues with an initial guess for  $(k, \omega_i)$ .<sup>7,11</sup> Table 2 below gives the eigenvalues  $(k, \omega_i)$  for the fixed frequency 200 Hz. These results have been obtained with the mean flow calculated for the diffuser length  $l/h = 13$ .

$k$ ( $m^{-1}$ )	$\omega/2\pi = (\omega_r + i\omega_i)/2\pi$
136x99 grid	
-5.002	200.000 - 3.740 <i>i</i>
-4.839	200.000 - 98.867 <i>i</i>
136x111 grid	
-5.024	200.000 + 3.834 <i>i</i>
-4.836	200.000 - 98.852 <i>i</i>

**Table 2 Numerical stability results.**

Two modes are solutions of the stability problem. Nevertheless, only the second one, the mode (200 - 98.86*i*), will be considered hereafter because the first mode, (200 - 3.74*i*) is completely dependent of the computational grid as shown in table 2 ( $\omega_i$  differs by 200%). Indeed, for this last mode the value and the sign of this  $\omega_i$  strongly depend on the grid. The physical mode ( $\omega = 200 - 98.8i$ ) is weakly dependant on  $x_u$  due to the fact that the mean flow is not strictly constant for  $x_u \leq x \leq x_e$ . More precisely if  $x_u/h \geq 11$ ,  $\omega_i$  will only be modified by a factor of 1%. Finally, the very small obtained value of  $k$  is in agreement with the experiment and is confirmed by a full 2D small perturbation analysis.<sup>13</sup>

### Computation of Shock Motion

As explained before, the fluctuations are proportional to the shock amplitude  $X$ . In order to determine a spectrum from the stability results, a normalisation must be introduced for the amplitude functions. As the fluctuating pressure spectrum is not known at the exit section, a uniform law is simply imposed :

$$|p_f(x_e)| = \varepsilon \bar{P}(x_e), \quad (22)$$

where  $\varepsilon$  is an arbitrary constant. The fluctuating pressure at the exit section is hence given as a fraction of the mean pressure. Finally, the shock motion spectrum is given by:

$$X(\omega) = \varepsilon \frac{\bar{P}(x_e)}{\bar{p}(x_e, \omega)} \quad (23)$$



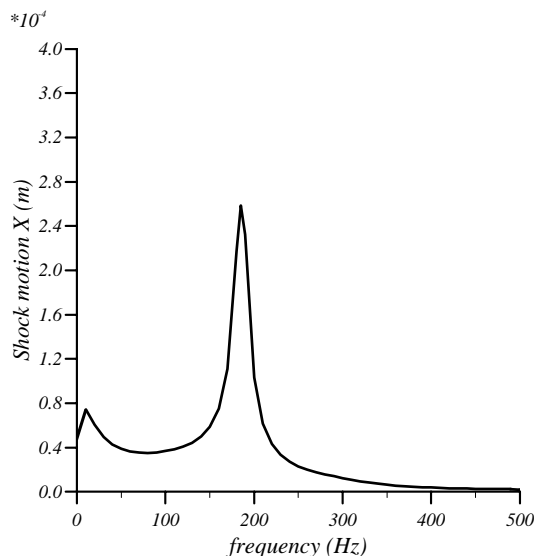
The constant  $c$  can be adjusted with an experimental data.

## Results

In order to validate the quasi-one-dimensional stability theory, the results are first compared with Sajben's experimental values and Hsieh's computations. The stability of the mean flow is then examined.

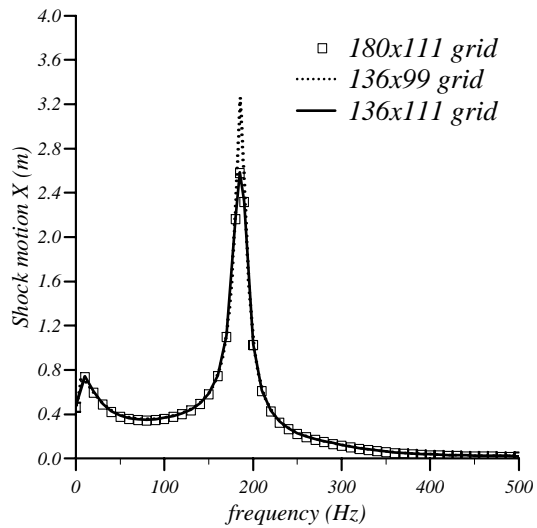
### Shock Motion Spectra

Figure 2 shows the experimental shock motion spectrum. It exhibits a well-defined peak close to 200 Hz, this means that the shock is more sensitive to excitations of frequencies around 200 Hz. The shock motion spectrum calculated by the one-dimensional stability analysis also provides a peak close to 200 Hz. Figure 8 presents this result. This spectrum has been calculated for the  $l/h = 13$  diffuser length and the mean flow calculated with the (136x111) grid. In order to evaluate the ro-



**Fig. 8 Shock motion spectrum,  $l/h = 13$ .**

bustness of this encouraging result, the stability analysis has been performed again but with the mean flow calculated with the (136x99) grid. Furthermore, just for the stability analysis, a fine mesh in  $x$  (180 points instead of 136) has been tested using a Tchebicheff polynomial interpolation for the mean flow. Figure 9 shows that the stability results do not depend either on the grid used for the stability or on the grid used for the computation of the mean flow. Concerning approximation (12), the shock motion spectra must be more or less independent of  $y$ . Figure 10 confirms this behaviour where  $j$  represents the vertical index for the  $y$ -line of the mesh. It seems that the quasi-one-dimensional



**Fig. 9 Robustness of shock motion spectrum.**

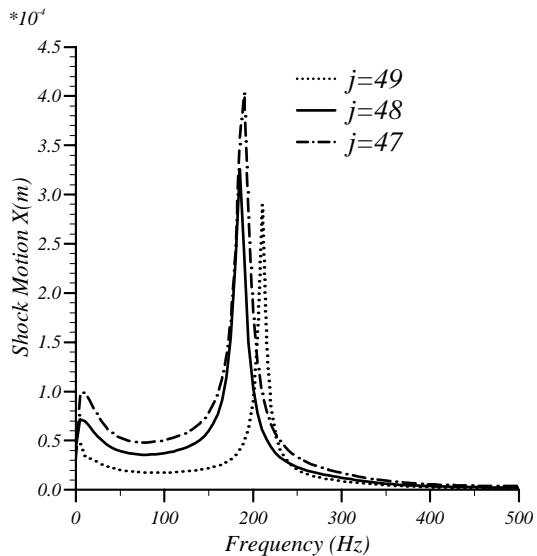


**Fig. 10  $y$ -dependence of shock motion spectrum.**

stability theory can be applied for Sajben's experiment.

Contrary to a forced calculation or it is imposed a periodic fluctuations, often monochromatic, in exit section, this study imposes a white noise in exit section or no frequency is privileged. The shock answer this white noise by selecting a very specific frequency, 200 Hz in our case. This method (the introduction of noise) is traditional when one wants to highlight the clean modes of a physical system. In our case the shock is an amplifier of noise. One fundamental parameter in the determination of the self-sustained oscillations frequency is the length of the diffuser. Different stability analyses have been performed for different lengths. Figure 11 shows the evolution of the observed frequency peak in the shock displacement spec-

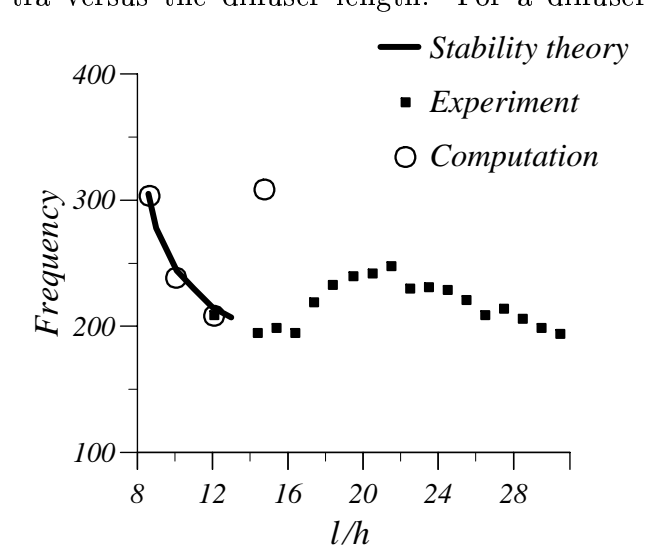


**Fig. 11 Frequency versus diffuser length.** length such as  $l/h = 13$ , the one-dimensional stability theory seems to be in good agreement with the experimental and numerical results. The four points with the label “computation” have been extracted from figure 3.<sup>3</sup>

#### Evolution of $\omega_i$ with the Frequency

The main objective of a linear stability analysis is to determine if the basic flow is stable with respect to infinitesimal perturbations. This stability is characterised by the sign of the temporal amplification growth rate  $\omega_i$ . Figure 12 shows the evolution of the temporal amplification coefficient  $\omega_i$ , it is always negative whatever the frequency is. Therefore, according to the stability definition, the mean flow is stable. Thus if the mean flow could be strictly not perturbed (at the exit section by some pressure fluctuations), no shock oscillation and no perturbation in the downstream zone could be observed. This could be verified experimentally by adding a second throat close to the exit section in order to eliminate any downstream excitation.

#### Pressure Fluctuation

This section is devoted to the comparison between Sajben’s experimental results and the temporal stability results for the amplitude and the phase of the pressure fluctuation. The results are illustrated in figures 13 and 14. A difference is observed, mainly close to the shock. However, it is important to note that the amplitude for the theoretical curve in figure 13 corresponds to the single frequency  $f = 200$  Hz, whereas the experimental amplitude covers a large frequency band.

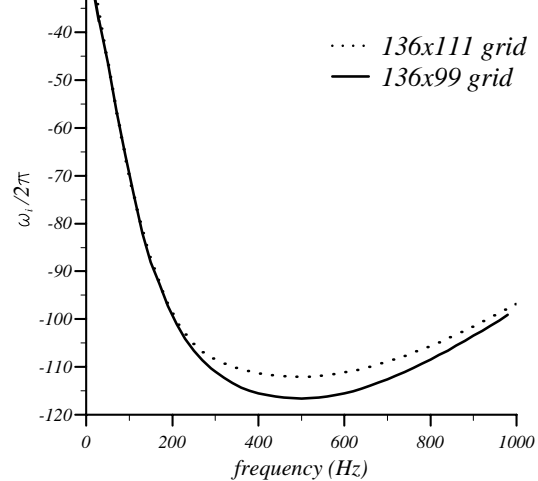


**Fig. 12 Variation of  $\omega_i$ .**

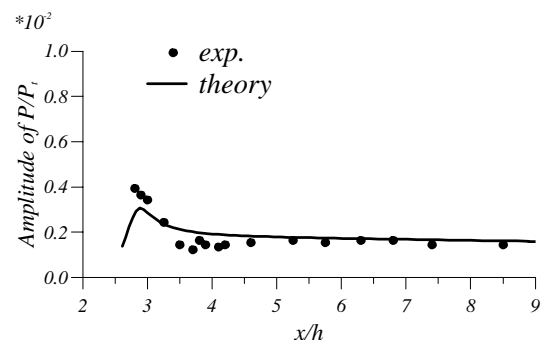


**Fig. 13 Amplitude of fluctuating pressure.**

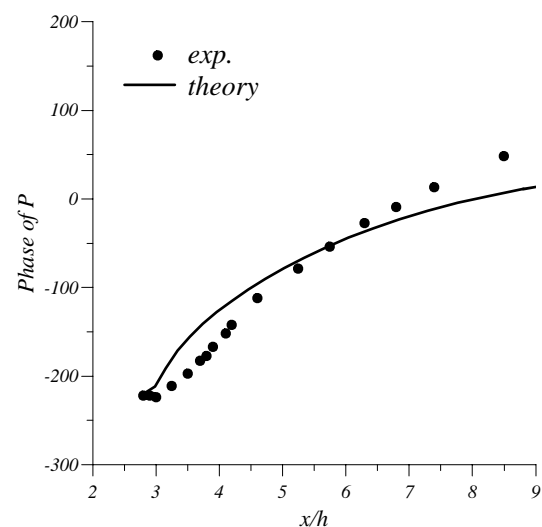


**Fig. 14 Phase of fluctuating pressure.**

On the other hand, concerning the phase variation (Fig. 14), there is a good agreement between stability and experimental results even if the theoretical results only concern one frequency ( $f = 200$  Hz).

## Summary and Conclusions

The goal of this paper is to present a new approaches based on the small perturbation technique in order to explain and to predict

the self-sustained shock oscillations observed in many diffusers: a 1D linear stability theory. In the Sajben's diffuser, the mean flow in the core region can be considered as a quasi-one-dimensional flow. Then an appropriate stability analysis has been developed in order to try to understand and to predict the self-sustained oscillations origin. The comparisons between experimental data, numerical simulations and linear theory have shown that the latter can provide the frequency of the shock oscillations. Finally, this study can give some new insight into the physical origin of the observed self-excited shock oscillations. Indeed, this analysis can show that at least in some cases, self-sustained shock oscillations can be predicted with an inviscid linear stability theory but with a mean flow computed with Navier-Stokes equations. The agreement between this theory and the experiment may suggest that the transverse waves carried by the boundary layer, in this case, are not the main mechanism to explain the observed self-sustained oscillations in transonic diffuser flow.

## Acknowledgements

This study has been carried out under contract n°93/CNES/3040 granted by the French Centre National d'Etudes Spatiales (CNES). The mean flow has been computed by R. Hallard (ONERA).

## References

<sup>1</sup>Sajben, M., Bogar, T. J., and Kroutil, J. C., "Characteristic Frequency and Length Scales in Transonic Diffuser Flow Oscillations," *AIAA paper 81-1291*, june, 1981.

<sup>2</sup>Liou, M. S., Coakley, T. J., and Bergmann, M. Y., "Numerical Simulation of Transonic Flows in Diffusers," *AIAA Paper 81-1240*, june, 1981.

<sup>3</sup>Hsieh, T. and Coakley, T. J., "Downstream Boundary Effects on the Frequency of Self-Excited Oscillations in Diffuser Flows," *AIAA paper 87-0161*, jan., 1987.

<sup>4</sup>Bogar, T. J., Sajben, M., and Kroutil, J. C., "Characteristic Frequencies of Transonic Diffuser Flow Oscillations," *AIAA Journal*, Vol. Vol. 21, No. 2, pp. 1232-1240, 1983.

<sup>5</sup>Sajben, M. and Bogar, T. J., "Unsteady Transonic Flow in a Two-Dimensional Diffuser : Interpretation of Experimental Results," Report MDC Q0779, Mac Donnell Douglas Corp., March 1982.

<sup>6</sup>Liou, M. S. and Coakley, T. J., "Numerical Simulation of Unsteady Transonic Flows in Diffusers," *AIAA Paper 82-1000*, june, 1982.

<sup>7</sup>Casalis, G., Hallard, R., Jouet, C., and Robinet, J.-C., "Calcul des caractéristiques stationnaires et instationnaires d'un écoulement décollé dans une tuyère, cas bidimensionnel," Convention CNES 933040, ONERA, Septembre 1996.

<sup>8</sup>Cambier, L., Darracq, D., Gazaix, M., Gullien, P., Jouet, C., and Toullec, L. L., "Améliorations récentes du code d'écoulements compressibles FLU3M," Progress and Challenges in CFD Methods and Algorithms, AGARD-CP-578, April 1996.

<sup>9</sup>Gleize, V. and Jouet, C., "Introduction de modèles de turbulence dans les codes Navier-Stokes: Applications à des écoulement bidimensionnels," *30ème Colloque d'Aérodynamique Appliquée, AAAF*, Octobre 1995.

<sup>10</sup>Kantrowitz, A., "The Formation and Stability of Normal Shock Waves in Channel Flows," Technical note 1225, NACA, March 1947.

<sup>11</sup>Casalis, G. and Robinet, J.-C., "Linear Stability Analysis in Transonic Diffuser Flows," *Aerospace Science and Technology*, Vol. Vol. 1, No. 1, pp. 37-47, 1998.

<sup>12</sup>Culick, F. E. C. and Rogers, T., "The Response of Normal Shocks in Diffusers," *AIAA Journal*, Vol. Vol. 21, No. 10, pp. 1382-1390, 1983.

<sup>13</sup>Robinet, J.-C. and Casalis, G., "Analyse de stabilité linéaire bidimensionnelle d'un écoulement de tuyère présentant un choc," Technical note RT. No. 98/5605.98, ONERA, juillet 1997.

## Appendix

To simplify the notations the following quantities  $\tilde{\omega}$  and  $\Omega$  are introduced :

$$\tilde{\omega} = \omega - k\bar{V} \quad \text{and} \quad \Omega = \sqrt{k^2(\bar{a}^2 - \bar{U}^2) - \tilde{\omega}^2}$$

The eigenvalues of  $\mathbf{C}^{-1}\mathbf{B}$  are:

$$l_1 = \frac{-i\tilde{\omega}\bar{U} + \bar{a}\Omega}{\bar{a}^2 - \bar{U}^2}, \quad l_2 = \frac{-i\tilde{\omega}\bar{U} - \bar{a}\Omega}{\bar{a}^2 - \bar{U}^2}, \quad l_3 = l_4 = \frac{i\tilde{\omega}}{\bar{U}}, \quad (24)$$

and the eigenvectors of these eigenvalues are :

$$\vec{V}_1 = \begin{bmatrix} \frac{1}{C_p k} (i\bar{U}l_1 + \tilde{\omega}) \\ \frac{\bar{p}}{k\bar{a}} (i\bar{U}l_1 + \tilde{\omega}) \\ -\frac{1}{k\bar{U}} i\bar{U}l_1 \\ 1 \end{bmatrix}, \quad \vec{V}_2 = \begin{bmatrix} \frac{1}{C_p k} (i\bar{U}l_2 + \tilde{\omega}) \\ \frac{\bar{p}}{k\bar{a}} (i\bar{U}l_2 + \tilde{\omega}) \\ -\frac{1}{k\bar{U}} i\bar{U}l_2 \\ 1 \end{bmatrix},$$

$$\vec{V}_3 = \begin{bmatrix} 1 \\ -\frac{\bar{p}}{\bar{T}} \\ 0 \\ 0 \end{bmatrix}, \quad \vec{V}_4 = \begin{bmatrix} 0 \\ 0 \\ 1 \\ -\frac{\tilde{\omega}}{k\bar{U}} \end{bmatrix}. \quad (25)$$

The matrix expressions of the differential system are :

$$\mathbf{C} = \begin{pmatrix} 0 & \bar{U} & \bar{p} & 0 \\ r\bar{p} & r\bar{T} & \bar{p}\bar{U} & 0 \\ 0 & 0 & 0 & \bar{p}\bar{U} \\ C_p \bar{U} \bar{p} & 0 & \bar{p}\bar{U}^2 & \bar{p}\bar{U}\bar{V} \end{pmatrix} \quad (26)$$

$$\begin{pmatrix} 0 & a_{12} & -\frac{\partial \bar{\rho}}{\partial x} & -iky\bar{\rho} \\ -r\frac{\partial \bar{\rho}}{\partial x} & a_{22} & \bar{\rho}a_{12} & 0 \\ -irk\bar{\rho} & a_{32} & -\bar{\rho}\frac{\partial \bar{V}}{\partial x} & i\bar{\rho}\tilde{\omega} \\ i(\tilde{\omega}C_p - r\omega)\bar{\rho} & -i\tilde{\omega}r\bar{T} & \bar{\rho}\bar{u}a_{12} & a_{44} \end{pmatrix} \quad (27)$$

with :

$$\begin{aligned} a_{12} &= i\tilde{\omega} - \frac{\partial \bar{U}}{\partial x} \\ a_{22} &= -\bar{U}\frac{\partial \bar{U}}{\partial x} - r\frac{\partial \bar{T}}{\partial x} \\ a_{32} &= -\bar{U}\frac{\partial \bar{V}}{\partial x} - irk\bar{T} \\ a_{44} &= i\tilde{\omega}\bar{\rho}\bar{V} - \bar{\rho}\bar{U}\frac{\partial \bar{V}}{\partial x} \end{aligned}$$

The vector and matrix expressions of algebraic system (18) are:

$$A = \begin{pmatrix} 0 & \bar{U}_1 & \bar{\rho}_1 & 0 \\ r\bar{\rho}_1 & \bar{U}_1 + r\bar{T}_1 & 2\bar{\rho}_1\bar{U}_1 & 0 \\ C_p & 0 & \bar{U}_1 & 0 \\ 0 & 0 & 0 & 1 \end{pmatrix} \quad (28)$$

$\xi = \xi_0 - \xi_1$  with :

$$\xi_i = \begin{pmatrix} \frac{\partial}{\partial x}(\bar{\rho}_i\bar{U}_i) + i(\omega - k\bar{V}_i)\bar{\rho}_i \\ \frac{\partial}{\partial x}(\bar{p}_i + \bar{\rho}_i\bar{U}_i^2) + 2i(\omega - k\bar{V}_i)\bar{\rho}_i\bar{U}_i \\ \frac{\partial}{\partial x}(C_p\bar{T}_i + \frac{1}{2}\bar{U}_i^2) + i(\omega - k\bar{V}_i)\bar{U}_i \\ \frac{\partial \bar{V}_i}{\partial x} + ik\bar{U}_i \end{pmatrix} \quad (29)$$